FDG and L-[1-^{11}C]-Tyrosine Imaging of Soft-Tissue Tumors Before and After Therapy

Annemieke C. Kole, Boudewijn E.C. Plaat, Harald J. Hoekstra, Willem Vaalburg and Willemina M. Molenaar

PET Center, Departments of Surgical Oncology and Pathology, Groningen University Hospital, Groningen, The Netherlands

This study was undertaken to investigate the relationship of PET using fluorodeoxyglucose (FDG) or L-[1-^{11}C]-tyrosine (TYR) with histopathologic findings in soft-tissue tumors, before and after therapy. Histopathologic parameters that were studied were tumor grade, mitotic rate, proliferation activity and amount of necrosis. **Methods:** PET with either FDG or TYR was performed in 55 patients with a lesion suspected to be a malignant soft-tissue tumor. In 28 patients, a second PET study was performed after therapy. Metabolic rate of glucose consumption (MRglc) and protein synthesis rate (PSR) were calculated. Histologic parameters were obtained from a biopsy specimen that was taken just after the first PET study and from the tumor remnant that was resected after therapy. **Results:** MRglc correlated with tumor grade (r = 0.71) and mitotic rate (r = 0.68) but not with proliferation or necrosis. After therapy, there was no longer a correlation with mitotic rate. PSR correlated with tumor grade (r = 0.53), mitotic rate (r = 0.73) and proliferation (r = 0.66). After therapy, correlation with mitosis and proliferation had improved, and a negative correlation was found between PSR and necrosis (r = −0.74). **Conclusion:** These results validate the use of both FDG and TYR to give an in vivo indication of histologic tumor parameters. However, FDG gives a better indication of tumor grade, whereas TYR is more accurate in predicting mitotic rate and proliferation, especially after therapy. FDG may therefore not be the most suited tracer for monitoring therapy. TYR might be more appropriate for that purpose.

Key Words: PET; histology; fluorodeoxyglucose; tyrosine; tumor

J Nucl Med 1999; 40:381–386

Although it seems obvious that a higher mitotic rate and proliferation require more energy, and that a loss of differentiation results in a less efficient and therefore higher metabolism, a clear correlation between metabolic and histologic parameters has not yet been demonstrated. With PET, the metabolism of tumors can be studied in vivo with radiopharmaceuticals. The radiopharmaceutical ^{18}F-fluoro-2-deoxy-D-glucose (FDG) is the most widely used PET tracer in oncology. With FDG, the metabolic rate of glucose consumption (MRglc) can be visualized and quantified (*1*). High glucose metabolism has been demonstrated with FDG PET in several types of soft-tissue tumors (STTs) (*2–3*). A relationship between the glucose consumption and the malignancy grade has been shown, but very little is known about the correlation of glucose consumption with other histopathologic tumor parameters.

Experimental studies have demonstrated that amino acid transport and protein synthesis rate (PSR) are increased in malignant cells (*4–5*). The majority of the amino acid PET studies in oncology have been performed with L-[methyl-^{11}C]-methionine (MET), which is relatively easy to synthesize. In our institute, L-[1-^{11}C]-tyrosine (TYR) is used for this purpose, because with TYR PET the PSR can be quantified, whereas MET uptake reflects amino acid transport rather than PSR (*6–7*). With TYR, several types of malignant tumors can be visualized (*8*). The relationship of PSR to histopathologic tumor parameters has not yet been elucidated. This study was undertaken to investigate the relationship of both FDG PET and TYR PET with histopathologic findings in STT, before and after therapy. STTs comprise 1% of all malignant tumors. Patients with an STT have a poor prognosis (50% 5-y survival). The estimation of malignancy of STT depends on mitosis and proliferation. Mitotic activity and proliferation have prognostic value (*9*). Histopathologic parameters that were studied were tumor grade, amount of necrosis, mitotic rate and proliferation activity, as assessed with Ki-67 labeling.

PATIENTS AND METHODS

Patients

The FDG PET group consisted of 30 patients, 13 men and 17 women (mean age 50 y, range 18–84 y) (Table 1). The TYR PET group consisted of 25 patients, 19 men and 6 women (mean age 55 y, range 25–83 y) (Table 2). All 55 patients were clinically and radiographically suspected of having a malignant STT, but histologic examination after PET revealed 46 malignant and 9 benign STTs. Conventional imaging consisted of plain radiography, bone scintigraphy, CT and/or MRI. All tumors were larger than 2 cm diameter. A biopsy to obtain a definite diagnosis was performed in all patients after the PET study, to avoid interference of wound healing on the PET signal. The study protocol was approved by the medical ethics committee of the Groningen University Hospital, and all patients gave informed consent.

To evaluate treatment response, 28 patients underwent a second PET study (17 FDG PET and 11 TYR PET) after therapy, which consisted of hyperthermic isolated limb perfusion (HILP) with tumor necrosis factor-α and melphalan, as described previously (*10*).

Received Feb. 11, 1998; revision accepted Aug. 4, 1998.

For correspondence or reprints contact: Willem Vaalburg, PhD, PET Center, Groningen University Hospital, PO Box 30.001, 9700 RB Groningen, The Netherlands.

TABLE 1
Characteristics of Patients Who Were Studied with FDG PET

Patient no.	Age	Sex	Histology	Tumor grade
1	59	F	Malignant fibrous histiocytoma	III
2	54	M	Malignant fibrous histiocytoma	III
3	39	F	Synovial sarcoma	III
4	40	F	Leiomyosarcoma	III
5	84	F	Sarcoma NOS	III
6	28	M	Sarcoma NOS	III
7	53	M	Malignant fibrous histiocytoma	II
8	80	M	Malignant fibrous histiocytoma	II
9	39	F	Malignant fibrous histiocytoma	II
10	65	F	Malignant peripheral nerve sheath tumor	II
11	62	M	Malignant peripheral nerve sheath tumor	II
12	43	M	Malignant peripheral nerve sheath tumor	II
13	50	F	Dedifferentiated liposarcoma	II
14	71	M	Liposarcoma	II
15	18	F	Rhabdomyosarcoma	II
16	56	F	Primitive peripheral neuroectodermal tumor	II
17	18	M	Extraskeletal myxoid chondrosarcoma	II
18	49	F	Sarcoma NOS	II
19	64	M	Sarcoma NOS	II
20	47	F	Myxoid malignant fibrous histiocytoma	I
21	39	F	Myxoid liposarcoma	I
22	44	F	Myxoid liposarcoma	I
23	48	F	Well-differentiated liposarcoma	I
24	57	M	Well-differentiated liposarcoma	I
25	56	M	Malignant fibrous histiocytoma	
26	38	M	Myxoma	0
27	21	M	Lymphangioma	0
28	43	F	Lipoma	0
29	82	F	Bursa	0
30	54	F	Ganglion	0

NOS = not otherwise specified.

PET Studies

FDG was routinely produced by a robotic system according to the procedure described by Hamacher et al. (*11*), with a radiochemical purity of more than 98%. TYR was produced by more than a modified microwave-induced Bücherer-Strecker synthesis (*12*). The radiochemical purity was more than 99%. A 951/31 ECAT positron scanner (Siemens/CTI, Knoxville, TN) was used for data acquisition. The scanner acquires 31 contiguous tomographic slices simultaneously over a total axial length of 10.8 cm and has a spatial resolution of 6 mm at full width half maximum.

Patients fasted overnight before the PET study. Serum glucose levels (and in case TYR PET was performed also tyrosine levels) were measured just before each PET session and were all within normal range. A 20-gauge needle was inserted into the radial artery while the patient was under local anesthesia. An intravenous cannula was inserted into the contralateral cephalic vein for the injection of the tracer. The patients were positioned supine in the scanner with the tumor in the field of view. A 20-min transmission scan was obtained to correct for attenuation of the photons by the body tissues. Then 185 MBq FDG or 370 MBq TYR was intravenously administered and sequential images were acquired at the level of the lesion by obtaining 16 frames from the time of injection through 50 min after injection. These include ten 30-s frames, three 5-min frames and three 10-min frames. For establishing the input function, blood samples were taken simultaneously from the arterial cannula (at 0.25, 0.5, 0.75, 1, 1.25, 1.5, 1.75, 2.25, 2.75, 3.75, 4.75, 7.5, 12.5, 17.5, 25, 35 and 45 min after injection). The same camera protocol was used for both tracers. The input function of the TYR studies was corrected for ^{11}C-labeled metabolites.

PET Data Analysis

The MRglc and the PSR of the lesions were calculated as described in detail previously (*13*). For calculating the MRglc or PSR, the 10 pixels with highest activity of the tumor were selected. When the lesion could not be visualized clearly, a region of interest was drawn around its location, based on MRI or CT findings. After therapy, the metabolism was calculated over the same volume as before therapy to avoid observer bias. Because it is known from a previous study that MRglc correlates better with malignancy grade than standardized uptake values, the latter were not calculated (*3*).

Histologic Examination

Histologic parameters that were compared with the PET findings before therapy were obtained from a biopsy specimen that was taken after the first PET study. Those compared with the PET

TABLE 2
Characteristics of Patients Who Were Studied with TYR PET

Patient no.	Age	Sex	Histology	Tumor grade
1	66	M	Malignant fibrous histiocytoma	III
2	67	F	Malignant fibrous histiocytoma	III
3	83	F	Malignant fibrous histiocytoma	III
4	26	F	Synovial sarcoma	III
5	45	M	Leiomyosarcoma	III
6	71	F	Fibrosarcoma	III
7	32	F	Malignant peripheral nerve sheath tumor	III
8	67	M	Pleiomorphic liposarcoma	III
9	75	M	Sarcoma NOS	III
10	69	F	Sarcoma NOS	III
11	76	M	Sarcoma NOS	III
12	68	M	Malignant fibrous histiocytoma	II
13	69	F	Malignant fibrous histiocytoma	II
14	25	M	Synovial sarcoma	II
15	49	M	Myxoid liposarcoma	II
16	69	M	Well-differentiated liposarcoma	I
17	49	F	Myxoid liposarcoma	I
18	58	M	Myxoid liposarcoma	I
19	48	M	Fibrosarcoma	I
20	43	M	Clear cell sarcoma	I
21	51	M	Malignant hemangiopericytoma	I
22	54	M	Lipoma	0
23	42	M	Lipoma	0
24	42	M	Benign peripheral nerve sheath tumor	0
25	47	M	Elastofibroma	0

NOS = not otherwise specified.

findings after therapy were obtained from the residual tumor that was resected as a whole, approximately 8 wk after HILP.

Histologic diagnosis was made on hematoxylin-eosin stained paraffin sections and additional immunohistologic stains, if necessary. All STTs were classified according to Enzinger and Weiss (*14*) and graded according to the system of Coindre et al. (*9*). Benign tumors were assigned tumor grade 0. The amount of necrosis was estimated on gross examination and microscopically. At least one section per centimeter of the largest tumor diameter was taken. The number of mitoses per 2 mm^2 (mitotic index) was counted in 15 adjacent fields on hematoxylin-eosin stained paraffin sections. Proliferation activity was assessed by Ki-67 labeling. Ki-67 is a nuclear antigen that is present during the whole cell cycle, except for the G0 and G1 phase and is therefore a measure of proliferation. For Ki-67 labeling, the monoclonal antibody MIB-1 (Immunotech S.A., Marseille, France) was used, which recognizes an epitope of the Ki-67 antigen. Ki-67 labeling was performed on paraffin sections (4 μm) according to a method modified from Shi et al. (*15*). In short, after being heated on a hot plate, slides were dewaxed in xylene and rehydrated in serial ethanol washes (100%, 96% and 70%). After being heated twice in an autoclave for 10 min at 110° C in 20 mmol/L citrate buffer (pH 6.0), slides were incubated with a 1:400 dilution of the antibody in maleate buffer (pH 7.4). The primary antibody was detected with a biotinylated secondary antibody followed by a streptavidine-alkaline phosphatase conjugate (ready-to-use link and label; Biogenex, San Ramon, CA). Final color was developed by the bromochlorindolyl-phosphate 4-nitroblue-tetrazoliumchloride method (Boehringer, Mannheim, Germany). For determining the Ki-67 labeling index (LI), we used ocular micrometry on a microscope with an eyepiece grid at ×400 magnification. In histologically viable areas, 15 fields were randomly selected. The positive and negative nuclei were counted. Endothelial cells, inflammatory cells and necrosis were excluded. The Ki-67 LI was defined as the number of positive nuclei divided by the total number of nuclei in each of the 15 fields. The mean Ki-67 LI of the 15 fields was calculated.

Statistical Analysis

To quantify the degree of correlation between the PET findings and the histologic parameters, a Spearman's (nonparametric parameters) or Pearson's correlation (parametric parameters) analysis was performed with SPSS statistical software (SPSS Inc., Chicago, IL). $P < 0.05$ was considered to be significant. A correction for multiple comparisons was made by adjusting the P level downward.

RESULTS

In the FDG PET group, PET was obtained in 29 patients before therapy (there was one technical failure). MRglc ranged from 0.6 to 99.1 μmol/100 g tissue/min. There were 6 grade III tumors, 12 grade II, 6 grade I and 5 grade 0 (Table 1). One tumor was not graded, because there was too little biopsy material for accurate grading. Necrosis ranged from 0% to 70%, mitotic rate from 0 to 25/2 mm^2 and the Ki-67 LI ranged from 1.2 to 38.4. After therapy, MRglc (range 7.4–44.4 μmol/100 g tissue/min), necrosis (range 0%–100%), mitotic rate (range 0–50/2 mm^2) and Ki-67 LI (range 0–37.1) were obtained in 17 patients.

Before therapy, a correlation was found between MRglc and tumor grade ($r = 0.71$) and mitotic rate ($r = 0.68$) (Figs. 1A and 2A). There was no correlation between the MRglc and Ki-67 LI (Fig. 3A) or the amount of necrosis either before or after therapy (Fig. 4A). After therapy, the correlation between MRglc and mitotic rate disappeared ($r = 0.18$).

In the TYR PET group, PET was obtained before therapy in 25 patients. PSR ranged from 0.13 to 5.66 nmol/kg tissue/min. There were 11 grade III tumors, 4 grade II, 6 grade I and 4 grade 0 (Table 2). Necrosis ranged from 0% to 80%, mitotic rate from 0 to 59/2 mm^2 and the Ki-67 LI ranged from 0.9 to 43.8. After therapy, PSR (range 0.50–2.79 nmol/kg tissue/min), necrosis (range 0%–59%), mitotic rate (range 0–40/2 mm^2) and the Ki-67 LI (range 0–33.0) were obtained in 11 patients.

Before therapy, a correlation was found between PSR and tumor grade ($r = 0.58$) (Fig. 1B), mitotic rate ($r = 0.73$) (Fig. 2B) and the Ki-67 LI ($r = 0.66$) (Fig. 3B). There was no correlation between the PSR and the amount of necrosis. After therapy, the correlation between PSR and mitotic rate ($r = 0.82$) (Fig. 2C) and between Ki-67 LI ($r = 0.87$) (Fig. 3C) had improved. There was now also a clear negative correlation between PSR and necrosis percentage ($r = -0.74$) (Fig. 4B).

DISCUSSION

This study demonstrates a clear correlation between both FDG PET and TYR PET on the one hand and several histopathologic tumor parameters on the other. This correlation exists even though the tumor metabolic activity as measured with PET is compared with histopathologic parameters from a biopsy specimen that may not be representative of the whole tumor.

In several previous PET studies with patients with STTs, a relationship was found between FDG uptake and malignancy grade (*2,3*). Low-grade tumors have lower FDG uptake than intermediate- and high-grade tumors. However, no significant difference was found between intermediate- and high-grade tumors. These results may elucidate this, because we did find a correlation between MRglc and mitotic rate but not between MRglc and necrosis. Malignancy grade was determined by mitotic rate, differentiation and the amount of necrosis (*9*). These parameters may have opposing effects on tumor metabolism as assessed with PET, especially in high-grade tumors. A high mitotic rate requires

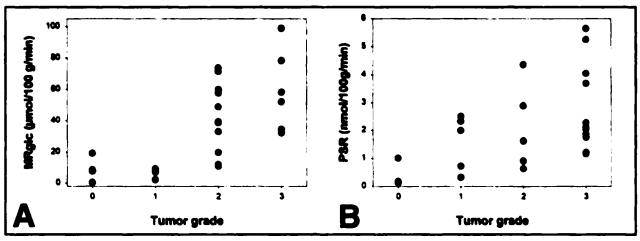

FIGURE 1. Metabolic rate of (A) glucose consumption (MRglc) and (B) protein synthesis rate (PSR) as measured with PET versus tumor grade. MRglc correlates better with tumor grade than PSR. Correlation coefficients are 0.71 and 0.58, respectively.

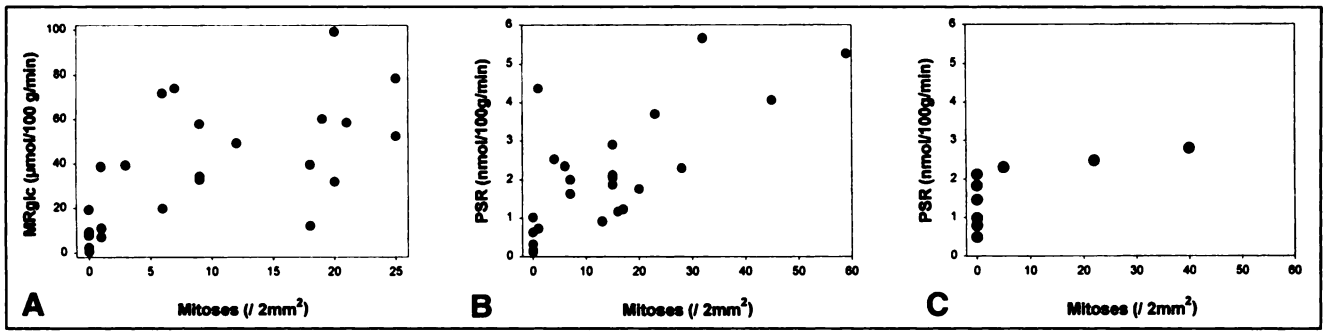

FIGURE 2. (A) Metabolic rate of glucose consumption (MRglc) and (B) protein synthesis rate (PSR) before and (C) after therapy as measured with PET versus mitotic activity. Correlation coefficients are 0.68, 0.73 and 0.82, respectively.

more energy and results in a high cell density, which in itself has been shown to correlate with FDG uptake in other tumor types (*16,17*). Differentiation is based on the resemblance to normal tissue, and poor differentiation is associated with more aggressive growth and a tendency to metastasize. Necrosis is a clear sign of aggressive and poorly controlled growth and will thus be found more in high-grade tumors with an increased rate of glucose consumption, but necrosis is not metabolically active. Therefore, with an increasing amount of necrosis, the average rate of glucose consumption of the tumor will decrease. Apparently, the same theory may be valid for TYR PET. However, the influence of necrosis on the tumor PSR appears to be stronger than on MRglc, because the correlation coefficient of PSR and tumor grade is lower ($r = 0.58$ versus $r = 0.71$) and after therapy, when necrosis becomes more prominent, a clear negative correlation between PSR and necrosis is shown. The latter may be explained by the fact that inflammatory cells that are frequently seen in necrotic areas and the reactive inflammatory tissue in the tumor rim after therapy also have a high MRglc, but no high PSR (*18–21*).

FDG uptake was shown to be related to proliferation in patients with intracranial tumors, bronchial carcinoma and head and neck tumors (*22–24*). However, we could not confirm this in patients with STTs. From the results from Minn et al. (*24*) and Watanabe et al. (*25*), it was suggested that the increase in glucose use in head and neck cancers is mainly needed for nucleic acid synthesis. However, larger changes in proliferation rate result in only moderate changes in FDG uptake (*26*). In in vitro studies, only a weak relationship of FDG uptake to proliferative activity was established (*16,27*). In patients with carcinoma of the hypopharynx, the relationship between FDG accumulation and the proliferative index was evident ($r = 0.80$), but only when the tumors with high and low FDG uptake were separated (*28*). These data suggest that another factor contributes to the uptake of FDG in tumors. This unknown factor might be the expression of an oncogene, which enhances glucose transport or density of glucose transporter proteins, or a simultaneously occurring inflammatory reaction.

In studies with patients with lung, breast or head and neck cancer, the uptake of the amino acid MET correlated well with the proliferative activity of the tumor (*29–31*). In in vitro studies, the relationship between amino acid uptake and proliferation was better than with FDG (*27*). We now validated these in vitro observations in the clinical situation in tumors with different growth characteristics using TYR PET. In two studies of patients with various brain tumors, no correlation was found between PSR as measured with TYR PET and proliferation (*32,33*). Although brain tumors and STTs are two entirely different entities, this suggests that there are also confounding factors influencing the PSR of tumors that are worth exploring.

Both MRglc and PSR correlated with mitotic rate. The

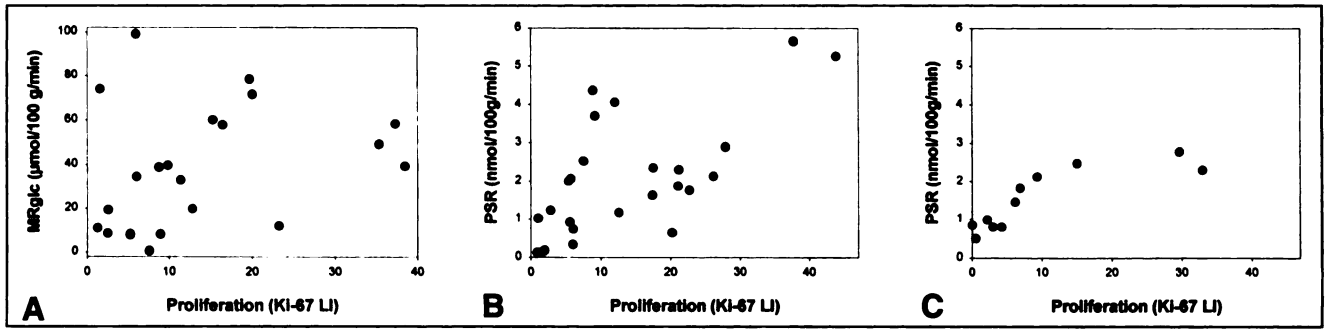

FIGURE 3. (A) Metabolic rate of glucose consumption (MRglc) and (B) protein synthesis rate (PSR) before and (C) after therapy as measured with PET versus proliferation activity. Correlation between MRglc and the Ki-67 labeling index (LI) is not significant. Correlation coefficient of PSR and proliferation is 0.66 before and 0.87 after therapy.

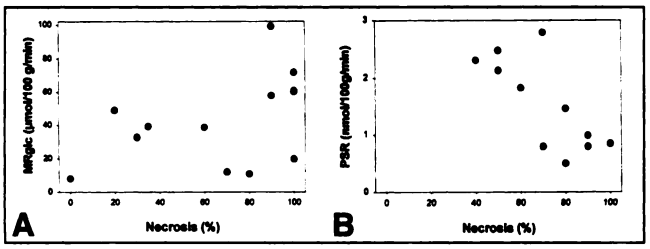

FIGURE 4. (A) Metabolic rate of glucose consumption (MRglc) and (B) protein synthesis rate (PSR) as measured with PET versus amount of necrosis after therapy. There is no significant correlation between MRglc and necrosis percentage, whereas there is clear negative correlation between PSR and necrosis ($r = -0.74$).

disappearance of the correlation between MRglc and mitotic rate after therapy might be influenced by the inflammatory reaction that was seen at all tumor sites after HILP. Except for tumor grade, TYR correlated better with all histologic tumor parameters than FDG, especially after therapy. FDG may therefore not be the most suited tracer for monitoring therapy. This was also the conclusion in a previous study that studied the value of FDG PET for monitoring treatment in similar patients (*34*). TYR PET may be more appropriate to monitor therapy. The first results of TYR PET for treatment evaluation that were reported recently, indeed confirmed less disturbance of inflammatory cells for TYR than for FDG, although with TYR a complete response could be distinguished from a partial response with 100% accuracy (*35*). Further studies investigating the value of TYR PET for monitoring therapy are therefore required.

CONCLUSION

This study demonstrates the correlation of tumor grade and mitotic rate with MRglc measured with FDG PET, whereas there was no correlation with the amount of necrosis and proliferation. A correlation was found between the PSR measured with TYR PET on the one hand and tumor grade, mitotic rate and proliferation on the other hand. After therapy, there was a clear negative correlation between the PSR and the amount of necrosis. FDG may not be the most suited tracer for monitoring therapy because of disturbing uptake by inflammatory cells. TYR PET might be more appropriate for that purpose.

ACKNOWLEDGMENT

We gratefully acknowledge the financial support by the Dutch Cancer Society (Koningin Wilhelmina Fonds) grants RuG 94–786 and RuG 95–1085.

REFERENCES

1. Patlak CS, Blasberg RG. Graphical evaluation of blood-to-brain transfer constants from multiple-time data. Generalizations. *J Cereb Blood Flow Metab.* 1985;5:584–590.
2. Adler LP, Blair HF, Makley JT, et al. Noninvasive grading of musculoskeletal tumors using PET. *J Nucl Med.* 1991;32:1508–1512.
3. Nieweg OE, Pruim J, van Ginkel RJ, et al. Fluorine-18-fluorodeoxyglucose PET imaging of soft-tissue sarcoma. *J Nucl Med.* 1996;37:257–261.
4. Isselbacher KJ. Sugar and amino acid transport by cells in culture—differences between normal and malignant cells. *N Engl J Med.* 1972;286:929–933.
5. Ishiwata K, Vaalburg W, Elsinga PH, Paans AMJ, Woldring MG. Metabolic studies with L-[1-^{14}C]tyrosine for the investigation of a kinetic model to measure protein synthesis rates with PET. *J Nucl Med.* 1988;29:524–529.
6. Ishiwata K, Kubota K, Murakami M, et al. Re-evaluation of amino acid PET studies: can the protein synthesis rates in brain and tumor tissues be measured in vivo? *J Nucl Med.* 1993;34:1936–1943.
7. Kubota R, Kubota K, Yamada S, et al. Methionine uptake by tumor tissue: a microautoradiographic comparison with FDG. *J Nucl Med.* 1995;36:484–492.
8. Kole AC, Pruim J, Nieweg OE, et al. PET with L-[1-carbon-11]-tyrosine to visualize of tumors and measure protein synthesis rates. *J Nucl Med.* 1997;38:191–195.
9. Coindre JM, Trojani M, Contesso G, et al. Reproducibility of a histopathologic grading system for adult soft tissue sarcoma. *Cancer.* 1986;58:306–309.
10. Eggermont AM, Schraffordt Koops H, Klausner JM, et al. Isolated limb perfusion with tumor necrosis factor and melphalan for limb salvage in 186 patients with locally advanced soft tissue extremity sarcomas. The cumulative multicenter European experience. *Ann Surg.* 1996;224:756–764.
11. Hamacher K, Coenen HH, Stocklin G. Efficient stereospecific synthesis of no-carrier-added ^{18}F-fluoro-2-deoxy-D-glucose using aminopolyether supported nucleophilic substitution. *J Nucl Med.* 1986;27:235–238.
12. Giron C, Luurtsema G, Vos MG, Elsinga PH, Visser GM, Vaalburg W. Microwave-induced preparation of ^{11}C amino acids via NCA-Bücherer-Strecker synthesis. *J Labelled Compd Radiopharm.* 1995;37:752–754.
13. Kole AC, Nieweg OE, Pruim J, et al. Standardized uptake values and the quantification of metabolism with ^{18}FDG and L-[1-^{11}C]-tyrosine PET in patients with breast carcinoma. *J Nucl Med.* 1997;38:692–696.
14. Enzinger FM, Weiss SW. *Soft Tissue Tumors.* St. Louis, MO: Mosby–Year Book; 1995.
15. Shi SR, Chaiwun B, Young L, Imam A, Cote RJ, Taylor CR. Antigen retrieval using pH 3.5 glycine-HCl buffer or urea solution for immunohistochemical localization of Ki-67. *Biotech Histochem.* 1994;69:213–215.
16. Higashi K, Clavo AC, Wahl RL. Does FDG uptake measure proliferative activity of human cancer cells? In vitro comparison with DNA flow cytometry and tritiated thymidine uptake. *J Nucl Med.* 1993;34:414–419.
17. Cremerius U, Striepecke E, Henn W, et al. ^{18}FDG-PET in intracranial meningiomas versus grading, proliferation index, cellular density and cytogenic analysis [in German]. *Nuklearmedizin.* 1994;33:144–149.
18. Kubota R, Yamada S, Kubota K, Ishiwata K, Tamahashi T, Ido T. Intratumoral distribution of fluorine-18-fluorodeoxyglucose in vivo: high accumulation in macrophages and granulation tissues studied by microautoradiography. *J Nucl Med.* 1992;33:1972–1980.
19. Reinhardt MJ, Kubota K, Yamada S, Iwata R, Yaegashi H. Assessment of cancer recurrence in residual tumors after fractionated radiotherapy: a comparison of fluorodeoxyglucose, L-methionine and thymidine. *J Nucl Med.* 1997;38:280–287.
20. Kubota K, Matsuzawa T, Fujiwara T, et al. Differential diagnosis of AH109A tumor and inflammation by radioscintigraphy with L-[methyl-^{11}C]methionine. *Jpn J Cancer Res.* 1989;80:778–782.
21. Sato T, Fujiwara T, Abe Y, et al. Double tracer whole body autoradiography using a short-lived positron emitter and a long-lived beta emitter [in Japanese]. *Radioisotopes.* 1989;38:7–12.
22. Di Chiro G, De La Paz RL, Brooks RA, et al. Glucose utilization of cerebral gliomas measured by (^{18}F) fluorodeoxyglucose and positron emission tomography. *Neurology.* 1982;32:1323–1329.
23. Lewis P, Griffin S, Marsden P, et al. Whole-body ^{18}F-fluorodeoxyglucose positron emission tomography in preoperative evaluation of lung cancer. *Lancet.* 1994;344:1265–1266.
24. Minn H, Joensuu H, Ahonen A, Klemi PJ. Fluorodeoxyglucose imaging: a method to assess the proliferative activity of human cancer in vivo. Comparison with DNA flow cytometry in head and neck tumors. *Cancer.* 1988;61:1776–1781.
25. Watanabe A, Tanaka R, Takeda N, Washiyama K. DNA synthesis, blood flow, and glucose utilization in experimental rat brain tumors. *J Neurosurg.* 1989;70:86–91.
26. Haberkorn U, Strauss LG, Reisser C, et al. Glucose uptake, perfusion, and cell proliferation in head and neck tumors: relation of positron emission tomography to flow cytometry. *J Nucl Med.* 1991;32:1548–1555.
27. Minn H, Clavo AC, Grenman R, Wahl RL. In vitro comparison of cell proliferation kinetics and uptake of tritiated fluorodeoxyglucose and L-methionine in squamous-cell carcinoma of the head and neck. *J Nucl Med.* 1995;36:252–258.
28. Strauss LG, Conti PS. The applications of PET in clinical oncology. *J Nucl Med.* 1991;32:623–648.

29. Miyazawa H, Arai T, Iio M, Hara T. PET imaging of non-small-cell lung carcinoma with carbon-11-methionine: relationship between radioactivity uptake and flow-cytometric parameters. *J Nucl Med.* 1993;34:1886–1891.
30. Leskinen-Kallio S, Någren K, Lehikoinen P, Ruotsalainen U, Joensuu H. Uptake of ^{11}C-methionine in breast cancer studied by PET. An association with the size of S-phase fraction. *Br J Cancer.* 1991;64:1121–1124.
31. Inoue T, Kim EE, Wrong FCL, et al. Comparison of fluorine-18-fluorodeoxyglucose and carbon-11-methionine PET in detection of malignant tumors. *J Nucl Med.* 1996;37:1472–1476.
32. Pruim J, Willemsen ATM, Molenaar WM, et al. Brain tumors: L-[1-C-11]tyrosine PET for visualization and quantification of protein synthesis rate. *Radiology.* 1995;197:221–226.
33. De Wolde H, Pruim J, Mastik MF, Koudstaal J, Molenaar WM. Proliferative activity in human brain tumors: comparison of histopathology and L-[1-^{11}C]tyrosine PET. *J Nucl Med.* 1997;38:1369–1374.
34. van Ginkel RJ, Hoekstra HJ, Pruim J, et al. FDG-PET to evaluate response to hyperthermic isolated limb perfusion for locally advanced soft-tissue sarcoma. *J Nucl Med.* 1996;37:984–990.
35. van Ginkel RJ, Kole AC, Nieweg OE, et al. L-1-[^{11}C]-tyrosine PET to evaluate response to hyperthermic isolated limb perfusion for locally advanced soft-tissue sarcoma and skin cancer. *J Nucl Med.* 1999;40:262–267.